



12-2019

Stability of a regular black holes thin-shell wormhole in Reissner-Nordstrom - De Sitter space-time

A. Eid

Imam Mohammad Ibn Saud Islamic University (IMSIU), Cairo University

Follow this and additional works at: <https://digitalcommons.pvamu.edu/aam>



Part of the [Other Physics Commons](#)

Recommended Citation

Eid, A. (2019). Stability of a regular black holes thin-shell wormhole in Reissner-Nordstrom - De Sitter space-time, *Applications and Applied Mathematics: An International Journal (AAM)*, Vol. 14, Iss. 2, Article 26.

Available at: <https://digitalcommons.pvamu.edu/aam/vol14/iss2/26>

This Article is brought to you for free and open access by Digital Commons @PVAMU. It has been accepted for inclusion in *Applications and Applied Mathematics: An International Journal (AAM)* by an authorized editor of Digital Commons @PVAMU. For more information, please contact hvkoshy@pvamu.edu.



Stability of a regular black holes thin-shell wormhole in Reissner-Nordstrom - De Sitter space-time

A. Eid

Department of Physics
Collage of Science
Imam Mohammad Ibn Saud Islamic University (IMSIU)
Riyadh, KSA

Department of Astronomy
Faculty of Science, Cairo University
Giza, Egypt
amaid@imamu.edu.sa; aeid06@yahoo.com;

Received: April 30, 2019; Accepted: September 15, 2019

Abstract

The dynamics regular black holes thin shell wormhole with a phantom energy equation of state in Reissner-Nordstrom - De sitter space-time is studied using the Darmois-Israel formalism. A mechanical stability analysis is carried out by using the standard perturbation method. The stable and unstable static solution depends on the suitable value of parameters.

Keywords: Cosmology; General relativity; Singularity; Phantom energy; Regular black holes; Astrophysics

MSC 2010 No.: 83C75; 83C57; 83C10; 83F05

1. Introduction

Regular black holes are the black holes which do not contain space-time singularities. Thin-shell wormholes can be constructed from the family of regular black holes (BHs) with regular (singularity-free) centers. The singularities are avoided in the interior of BHs while the horizon is indeed formed. Bardeen (1968) was the first one proposed a regular BH solution with specific ratio of mass and charge. Ayon-Beato and Garcia (1998) investigated another regular BH coupled with nonlinear electrodynamics (known as ABG black holes). Hayward (2006) analyzed a similar type of regular BHs. Eiroa and Sendra (2013) studied the regular phantom black holes as gravitational lenses. Sharif and Iftikhar (2015) studied the dynamics of scalar thin-shell for a class of regular black holes. Ghaffarnejad et al. (2018)

discussed the gravitational lenses of charged Ayon-Beato-Garcia black holes and nonlinear effects of Maxwell field. Borkar and Gayakwad (2014) discussed the evaluation of Schwarzschild exterior and interior solutions in Bimetric theory of gravitation.

A mechanical stability analysis of shells was discussed by many authors. Kim (1992) analyzed Schwarzschild- De Sitter wormholes, using the cut-and-paste techniques. Poisson and Visser (1995) discussed a thin-shell wormhole by pasting together two copies of the Schwarzschild metric. Garcia et al. (2012) analyzed generic thin-shell traversable wormholes in standard general relativity. Furthermore, Kuhfittig (2014) discussed the stability of thin-shell wormholes. Eiroa and Simeone (2011) analyzed the stability of charged thin-shells. Rahaman et al. (2010) studied the thin-shell wormholes from regular charged black holes. Eid (2018) has studied Schwarzschild-De Sitter TSW supported by a generalized cosmic chaplygin gas. Furthermore, Uchikata et al. (2012) investigated new solutions of charged regular black holes and their stability. Halilsoy et al. (2014) studied stability of regular Hayward wormhole configurations. Sharif and Mumtaz (2016) have also discussed the stability of regular Hayward thin-shell wormholes.

In this paper, the stability of thin-shell wormhole (TSW) from regular black holes (RBHs) supported by phantom equation of state is discussed. In Section 2, the dynamics of a regular thin-shell wormhole in the framework of Darmois–Israel formalism is derived. The stability analysis of regular thin-shell wormhole with phantom energy equation of state is discussed in Section 3, and a general conclusion is finally given in Section 4.

2. Dynamics of a radiating thin shell wormhole

The space-time outside and inside the shell is described by:

$$ds_{\pm}^2 = -F_{\pm}(r) dt^2 + F_{\pm}^{-1}(r) dr^2 + r^2(d\theta^2 + \sin^2\theta d\phi^2), \quad (1)$$

where $F_{\pm}(r)$ are given by:

$$F_{+}(r) = 1 - \frac{2m}{r} + \frac{q^2}{r^2}, \quad r > a(\tau),$$

for the Reissner-Nordstrom (RN) space-time outside the shell (denoted by suffix +), and

$$F_{-}(r) = 1 - \frac{r^2}{L^2}, \quad r < a(\tau),$$

For De sitter space-time inside the shell (denoted by suffix -), where m is the gravitational mass, q is the charge density, $L = \sqrt{3/\Lambda}$, and Λ is the gravitational constant. The intrinsic metric at the throat Σ is given by:

$$ds^2 = -d\tau^2 + a(\tau) dr^2 + r^2(d\theta^2 + \sin^2\theta d\phi^2), \quad (2)$$

with the proper time τ of the shell. The time evolution of the shell $a(\tau)$ is described by equation $r = a(\tau)$. Applying the cut- and- paste technique, Israel (1966), to matter on Σ , the

extrinsic curvatures associated with the two sides of the shell are:

$$K_{ij}^{\pm} = -n_{\gamma}^{\pm} \left(\frac{\partial^2 x^{\gamma}}{\partial \xi^i \partial \xi^j} + \Gamma_{\alpha\beta}^{\gamma} \frac{\partial x^{\alpha}}{\partial \xi^i} \frac{\partial x^{\beta}}{\partial \xi^j} \right) \Big|_{\Sigma}, \quad (3)$$

where n_{γ}^{\pm} are the unit normal 4-vector to Σ in M , with $n_{\mu}n^{\mu} = 1$, and $n_{\mu}e_i^{\mu} = 0$. The Lanczos equations are given by:

$$t_{ij} = \frac{-1}{8\pi} \left([K_{ij}] - [K]g_{ij} \right), \quad (4)$$

where $[K]$ is the trace of $[K_{ij}] = K_{ij}^+ - K_{ij}^-$ and t_{ij} is the surface stress-energy tensor on Σ . The Lanczos equations are reduced to:

$$\sigma = \frac{-1}{4\pi} [K_{\theta}^{\theta}], \quad (5)$$

$$p = \frac{1}{8\pi} \left([K_{\tau}^{\tau}] + [K_{\theta}^{\theta}] \right), \quad (6)$$

where σ and p are the energy density and pressure. The extrinsic curvatures are:

$$K_{\tau\tau}^{\pm} = \mp \frac{2\ddot{a} + F'_{\pm}(a)}{2\sqrt{\dot{a}^2 + F_{\pm}(a)}}, \quad K_{\theta\theta}^{\pm} = \pm \frac{1}{a} \sqrt{\dot{a}^2 + F_{\pm}(a)} \quad (7)$$

where the dot and the prime denote derivatives with respect to τ and r , respectively. The Lanczos equations (5), (6), with the extrinsic curvature equations (7), are given by:

$$4\pi a\sigma = \sqrt{\dot{a}^2 + F_+(a)} - \sqrt{\dot{a}^2 + F_-(a)}, \quad (8)$$

$$p = p_{\theta} = p_{\phi} = \left[\frac{2a\ddot{a} + 2\dot{a}^2 + 2F(a) + aF'(a)}{8a\pi \sqrt{\dot{a}^2 + F(a)}} \right]_{-}^{+}. \quad (9)$$

In the case of dust $p = 0$, the equation (8), where $4\pi a^2\sigma = M$ is written in the form:

$$\sqrt{\dot{a}^2 + F_-(a)} - \sqrt{\dot{a}^2 + F_+(a)} = \frac{M}{a}, \quad (10)$$

which is the motion equation obtained from the Lanczos equation. The phantom energy equation of state is given by:

$$p = -\omega\sigma, \quad (11)$$

where $\omega > 0$ is a positive constant. Inserting equations (8) and (9) into equation (11), the dynamical equation becomes:

$$(2a\ddot{a} + 2\dot{a}^2(1 - \omega)) \left(\sqrt{\dot{a}^2 + F_-} - \sqrt{\dot{a}^2 + F_+} \right)$$

$$\begin{aligned}
& +2(1-\omega)\left(F_+\sqrt{\dot{a}^2+F_-}-F_-\sqrt{\dot{a}^2+F_+}\right) \\
& +a\left(F'_+\sqrt{\dot{a}^2+F_-}-F'_-\sqrt{\dot{a}^2+F_+}\right)=0.
\end{aligned} \tag{12}$$

This differential equation describes the evolution of the wormhole throat. It is convenient to define the parameter space of the problem using m, ω, q and Λ as free parameters.

3. Linearized stability analyses

The dynamical equation (12) for the static solution (where $\ddot{a} = \dot{a} = 0$), becomes:

$$2(1-\omega)(F_+\sqrt{F_-}-F_-\sqrt{F_+})+a_0(F'_+\sqrt{F_-}-F'_-\sqrt{F_+})=0. \tag{13}$$

In the static case the surface energy density and pressure becomes:

$$4\pi a_0 \sigma = \sqrt{F_-(a_0)} - \sqrt{F_+(a_0)}, \tag{14}$$

and

$$p = p_\theta = p_\phi = \left[\frac{2F(a_0) + aF'(a_0)}{8\pi a_0 \sqrt{F(a_0)}} \right]_{-}^{+}. \tag{15}$$

The conservation equation with (4) and (11) can be written as:

$$\frac{d}{d\tau} \sigma A + p \frac{dA}{d\tau} = 0, \tag{16}$$

where $A = 4\pi a^2$ is the area of the wormhole throat, and can be written in the form:

$$a\sigma' = -2(\sigma + p). \tag{17}$$

The dynamical equation of motion of the thin-shell wormhole, from equation (8), becomes:

$$\dot{a}^2 + V(a) = 0, \tag{18}$$

where $V(a)$ is known as the effective potential function,

$$V(a) = \frac{1}{2}(F_+ + F_-) - 4\pi^2 a^2 \sigma^2 - (64\pi^2 a^2 \sigma^2)^{-1} (F_+ - F_-)^2, \tag{19}$$

and can be written in the form:

$$V(a) = 1 - \left(\frac{\frac{a^3}{L^2} + \frac{q^2}{a} - 2m}{2M} \right)^2 - \left(\frac{M}{2a} \right)^2 - \frac{a^2}{2L^2} + \frac{q^2}{2a^2} - \frac{m}{a}. \tag{20}$$

Its derivative is:

$$V'(a) = \frac{1}{2}(F'_+ + F'_-) + 8\pi^2 a \sigma (\sigma + 2p) - \frac{(F_+ - F_-)}{32\pi^2 a^2 \sigma^2} \left[(F'_+ - F'_-) + \frac{(F_+ - F_-)(\sigma + 2p)}{a\sigma} \right]. \quad (21)$$

Taking the first derivative of equation (11) and using (17), we obtain:

$$\sigma' + 2p' = \sigma'(1 - 2\omega). \quad (22)$$

The Taylor series expansion of $V(a)$ up to second order around a_0 , is given by:

$$V(a) = \sum_{n=0}^2 b_n (a - a_0)^n, \quad b_n = \frac{V^{(n)}(a_0)}{n!}. \quad (23)$$

The surface energy density and the pressure (14), (15) can be written in the form:

$$\sigma_0 = \frac{-1}{4\pi a_0} \left(\sqrt{1 - \frac{2m}{a_0} + \left(\frac{q}{a_0}\right)^2} - \sqrt{1 - \frac{1}{3}\Lambda a_0^2} \right), \quad (24)$$

and

$$p_0 = \frac{1}{4\pi a_0} \left[\frac{1 - \frac{m}{a_0}}{\sqrt{1 - \frac{2m}{a_0} + \left(\frac{q}{a_0}\right)^2}} - \frac{1 - \frac{2}{3}\Lambda a_0^2}{\sqrt{1 - \frac{1}{3}\Lambda a_0^2}} \right]. \quad (25)$$

The stability of static solutions at $a = a_0$ requires $V(a_0) = 0$, and $V'(a_0) = 0$, while the second derivatives $V''(a_0)$ becomes:

$$\begin{aligned} V''(a) = & \frac{1}{2}(F''_+ + F''_-) + 8\pi^2 [a\sigma(\sigma' + 2p') - (\sigma + 2p)^2] - \frac{(F_+ - F_-)}{32\pi^2 a^2 \sigma^2} \\ & \left[(F''_+ - F''_-) + \frac{(F_+ - F_-)(\sigma' + 2p')}{a\sigma} + \frac{(F'_+ - F'_-)(\sigma + 2p)}{a\sigma} + \frac{(F_+ - F_-)(\sigma + 2p)^2}{a^2 \sigma^2} \right] \\ & - \frac{1}{32\pi^2 a^3 \sigma^3} [(F'_+ - F'_-)a\sigma + 2(F_+ - F_-)(\sigma + 2p)] \\ & \left[(F'_+ - F'_-) + \frac{(F_+ - F_-)(\sigma + 2p)}{a\sigma} \right]. \end{aligned} \quad (26)$$

The thin-shell wormhole is stable under radial perturbations if and only if $V''(a_0) > 0$, and unstable if $V''(a_0) < 0$. By letting $V''(a_0) = 0$, the squared sound speed β^2 is given by:

$$\beta^2 = -1 + \frac{16\pi^2 a^4 \sigma^2}{2(1-2\omega)[(16\pi^2 a^2 \sigma^2)^2 - (F_+ - F_-)^2]} \left\{ (F_+'' + F_-'') - 16\pi^2 (\sigma + 2p)^2 \right. \\ \left. - a^2 [(F_+'' - F_-'')(F_+ - F_-) + (F_+' - F_-')^2] \right. \\ \left. - \frac{1}{\sigma^2} [3(F_+ - F_-)^2 (\sigma + 2p)^2 + 4a\sigma(F_+' - F_-')(F_+ - F_-)(\sigma + 2p)] \right\}. \quad (27)$$

Variation of β^2 versus a_0 is plotted in Figures 1-5 with different values of m, ω, Λ and q as free parameters.

4. Discussion

The stability regions have been plotted in the form of parameter β^2 versus R_0 . Figures 1-5 show the stability regions with different values of free parameters in phantom energy EoS. Therefore, the stability region happens when the charge $|q|$ is slightly smaller than the mass. This result is similar to the result of Eid (2017). Also, the stability regions belong to the case of negative and positive cosmological constant by varying its range for fixed value of mass is discussed. This shows that the physical relevance of negative and positive cosmological constant on wormhole stability; these stable configurations are similar to Eiroa (2008), but do not correspond to the range $0 < \beta^2 \leq 1$ for different values of the parameters. Eid (2017) discussed the stability of TSWs in Born-infield theory supported by polytropic phantom energy.

5. Conclusions

The dynamics of regular black holes TSW with a phantom energy equation of state is derived. A mechanical stability analysis of regular BHs TSW about the static solution has been carried out. The RBHs TSW is stable under radial perturbations if and only if $V''(a_0) > 0$, while for $V''(a_0) < 0$, the static solution is unstable. The output of a RTSW can be a stable or unstable, depending on the suitable value of parameters m, ω, Λ and q .

Acknowledgement

The researcher acknowledges the Deanship of scientific Research at Imam Mohammad Ibn Saud Islamic University (IMSIU), Saudi Arabia, for financing this project under the grant number (381210).

REFERENCES

Ayon-Beato, E. and Garcia, A. (1998). Regular black hole in general relativity coupled to nonlinear electrodynamics, Phys. Rev. Lett., Vol.80, No. 23, pp. 5056-5059.

- Bardeen, J.M. (1968). Non-singular General Relativistic Gravitational Collapse: In Proceeding of the international conference GR5, Tbilisi, USSR, Georgia, pp. 174-180.
- Borkar, M. S., and Gayakwad, P.V.(2014). Evaluation of Schwarzschild exterior and interior solutions in Bimetric theory of gravitation, *Appl. Appl. Math.*, Vol.9, No. 1, pp. 260-271.
- Eid, A. (2017). Stability of TSWs in Born-infield theory supported by polytropic phantom energy, *Journal of the Korean Physical Society*, Vol.70, pp. 436-441.
- Eid, A. (2017). Stability of charged TSWs supported by polytropic gas, *New Astronomy*, Vol.53, pp. 6-11.
- Eid, A. (2018). Schwarzschild de Sitter TSW supported by a generalized cosmic Chaplygin gas, *Grav. Cos.*, Vol. 24, pp. 378-383.
- Eiroa, E. F. (2008). Stability of thin-shell wormholes with spherical symmetry, *Phys. Rev. D*, Vol.78, pp. 024018-024024.
- Eiroa, E. F., and Simeone, C. (2011). Stability of charged thin-shells, *Phys. Rev. D.*, Vol.83, pp. 1040091-1040096.
- Eiroa, E. F., and Sendra, C. M. (2013). Regular phantom black holes as gravitational lenses, *Phys. Rev. D.*, Vol.88, pp. 1030071–1030079.
- Garcia, N. M., Lobo, F. S. N., and Visser, M. (2012). Generic spherically symmetric dynamic thin-shell traversable wormholes in standard general relativity, *Phys. Rev. D.*, Vol.86, pp. 04402601-04402620.
- Ghaffarnejad, H., Amirmojahedi, M., and Niad, H. (2018). Gravitational Lensing of Charged Ayon-Beato-Garcia black holes and nonlinear effects of Maxwell fields, *Advances in High Energy Physics*, ID 3067272, pp. 1-19.
- Halilsoy, M., Ovgunand, A., and Mazharimousavi, S. H. (2014). Thin shell wormholes from the regular Hayward black hole, *Eur. Phys. J.* , Vol.74, pp. 27961-27967.
- Hayward, S. A. (2006). Formation and evaporation of nonsingular black holes, *Phys. Rev. Lett.*, 96, pp. 0311011-0311014.
- Israel, W. (1966). Singular hypersurfaces and thin shells in general relativity, *Nuovo Cimento B.*, 44, pp. 1-14.
- Kim, S. W. (1992). Schwarzschild-de Sitter type wormhole, *Phys. Lett. A.*, 166, pp. 13-16.
- Kuhfittig, P. K. F. (2014). On the stability of thin-shell wormholes, *J. Mod. Phys.*, 7, pp. 111-119.
- Poisson, E., and Visser, M. (1995). Thin-shell wormholes: Linearization stability, *Phys. Rev. D*.52, pp.7318-7321.
- Rahaman, F., Rahman, K. A., Rakib, S. A., and Kuhfittig, P. K.F. (2010). Thin shell Wormholes from regular charged black holes, *Int. Jour. Theor. Phys.*, 49, pp.2364-2378.
- Sharif, M., and Iftikhar, S. (2015). Dynamics of scalar thin shell for a class of regular black holes, *Astrophys. Space Sci.*, 356, pp.89-101.
- Sharif, M., and Mumtaz, S. (2016). Stability of the regular Hayward thin shell wormholes, *Advanced High Energy Phys.*, ID. 2868750, pp.1-13.
- Uchikata, N., Yoshida, S., and Futamase, T. (2012). New solutions of charged regular black holes and their stability, *Phys. Rev. D*, 86, pp. 0840251-0840258.

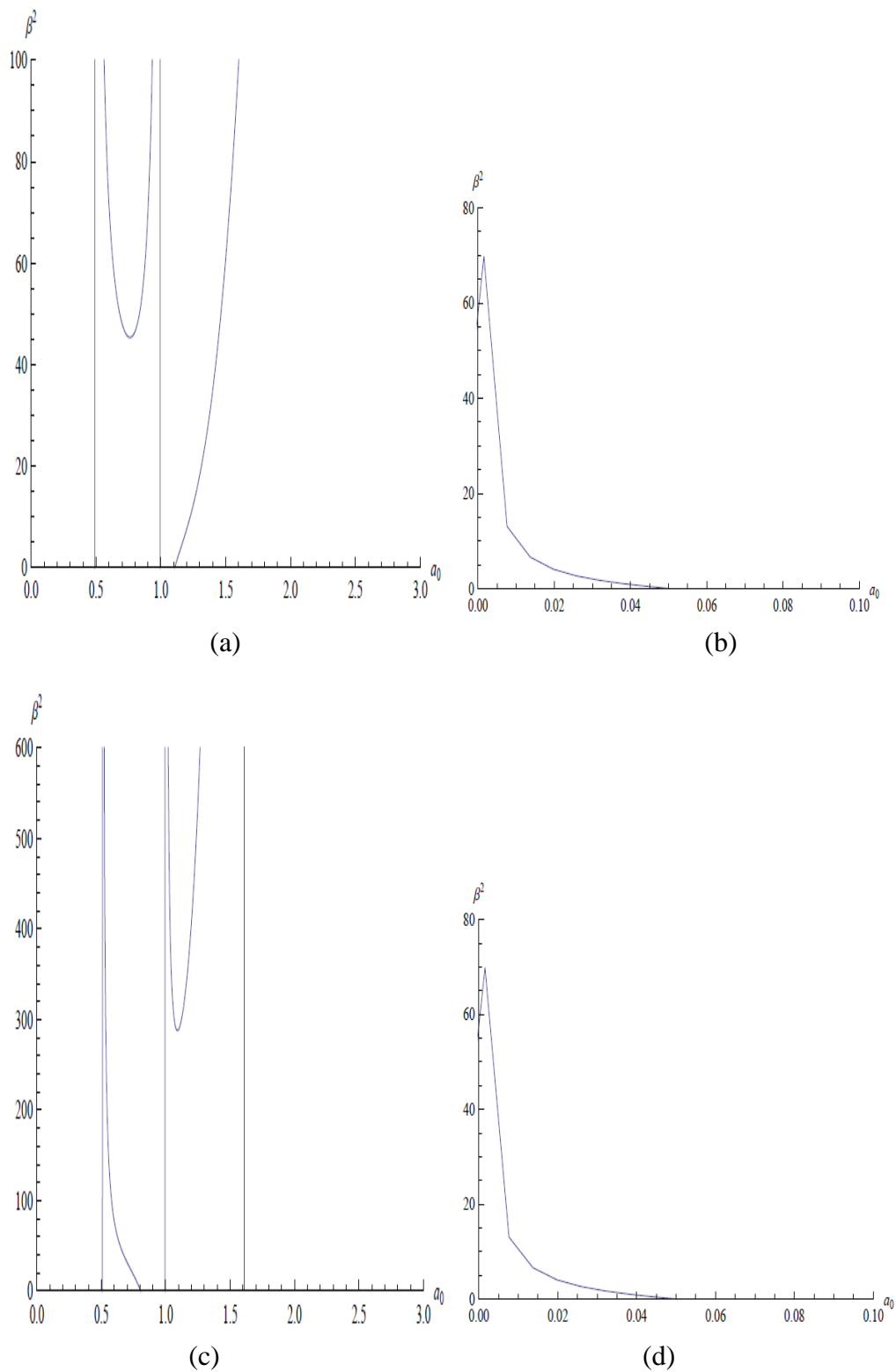


Figure 1. Stability regions TSW corresponding to $\omega = 1$ and the fixed value $m = 1$:
 (a) $\Lambda = -1, q = 1$, (b) $\Lambda = -1, q = 0.5$, (c) $\Lambda = 1, q = 1$, (d) $\Lambda = 1, q = 0.5$

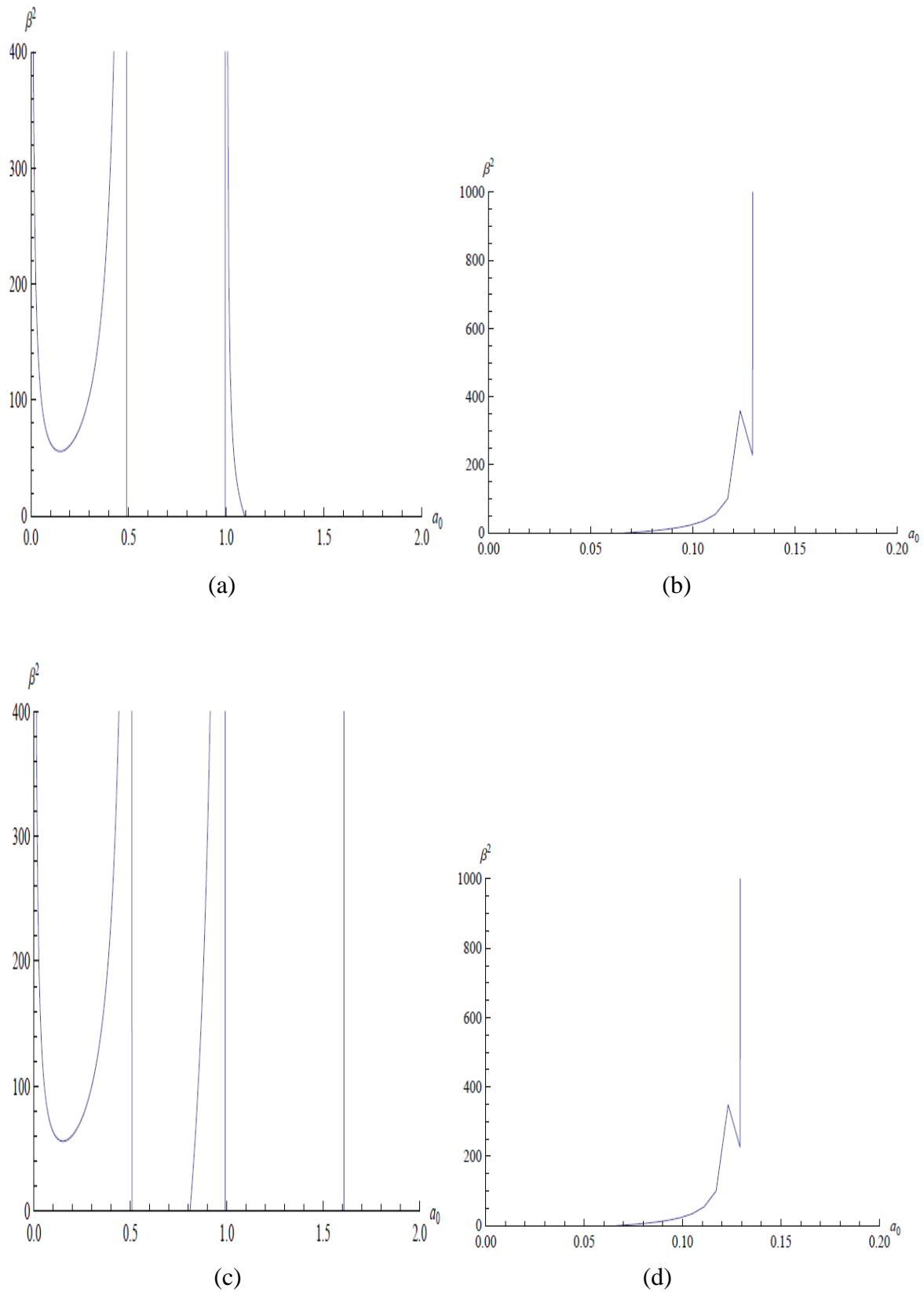


Figure 2. Stability regions TSW corresponding to $\omega = 0.4$ and the fixed value $m = 1$:
 (a) $\Lambda = -1, q = 1$, (b) $\Lambda = -1, q = 0.5$, (c) $\Lambda = 1, q = 1$, (d) $\Lambda = 1, q = 0.5$

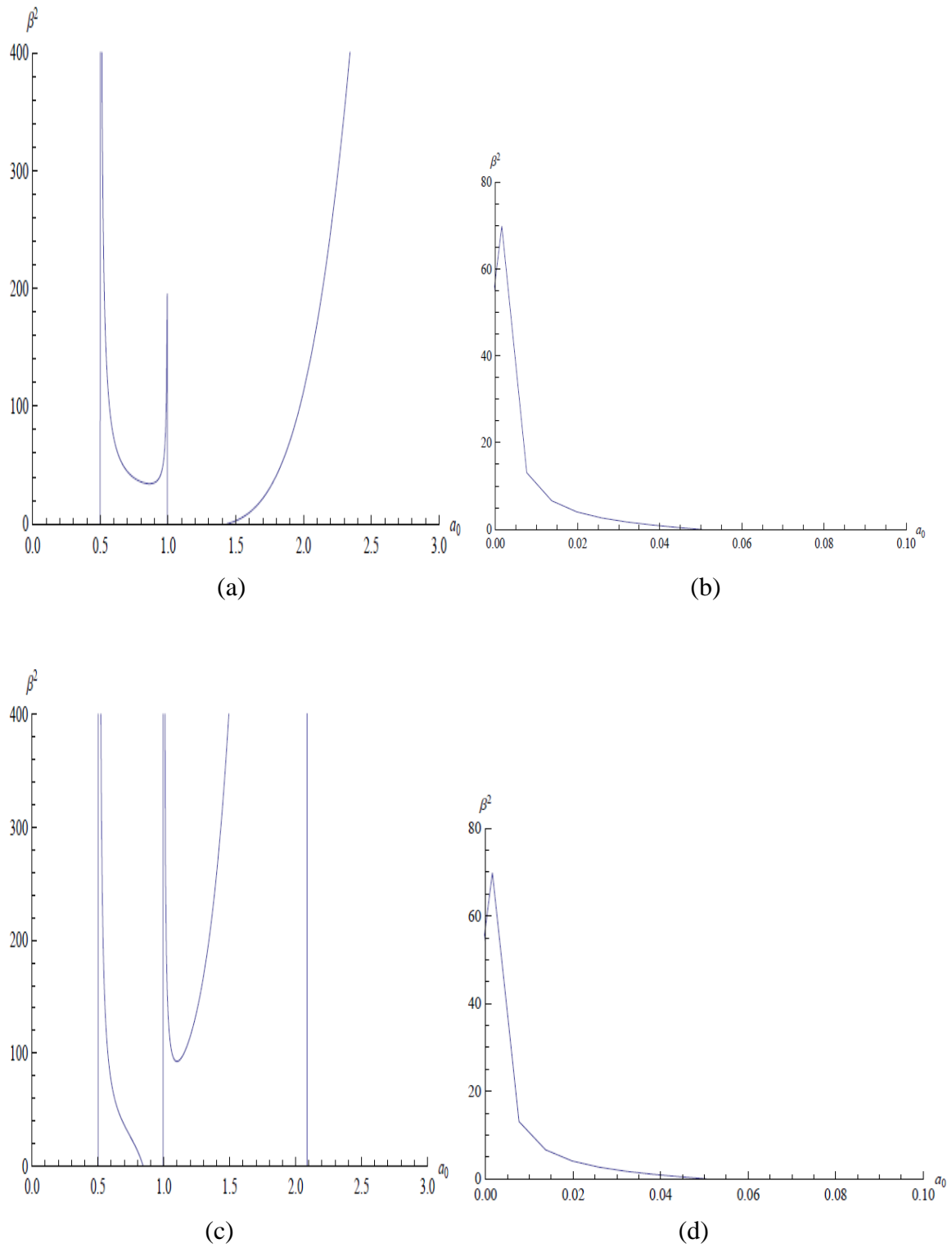


Figure 3. Stability regions TSW corresponding to $\omega = 1$ and the fixed value $m = 1$:
 (a) $\Lambda = -0.5, q = 1$, (b) $\Lambda = -0.5, q = 0.5$, (c) $\Lambda = 0.5, q = 1$, (d) $\Lambda = 0.5, q = 0.5$

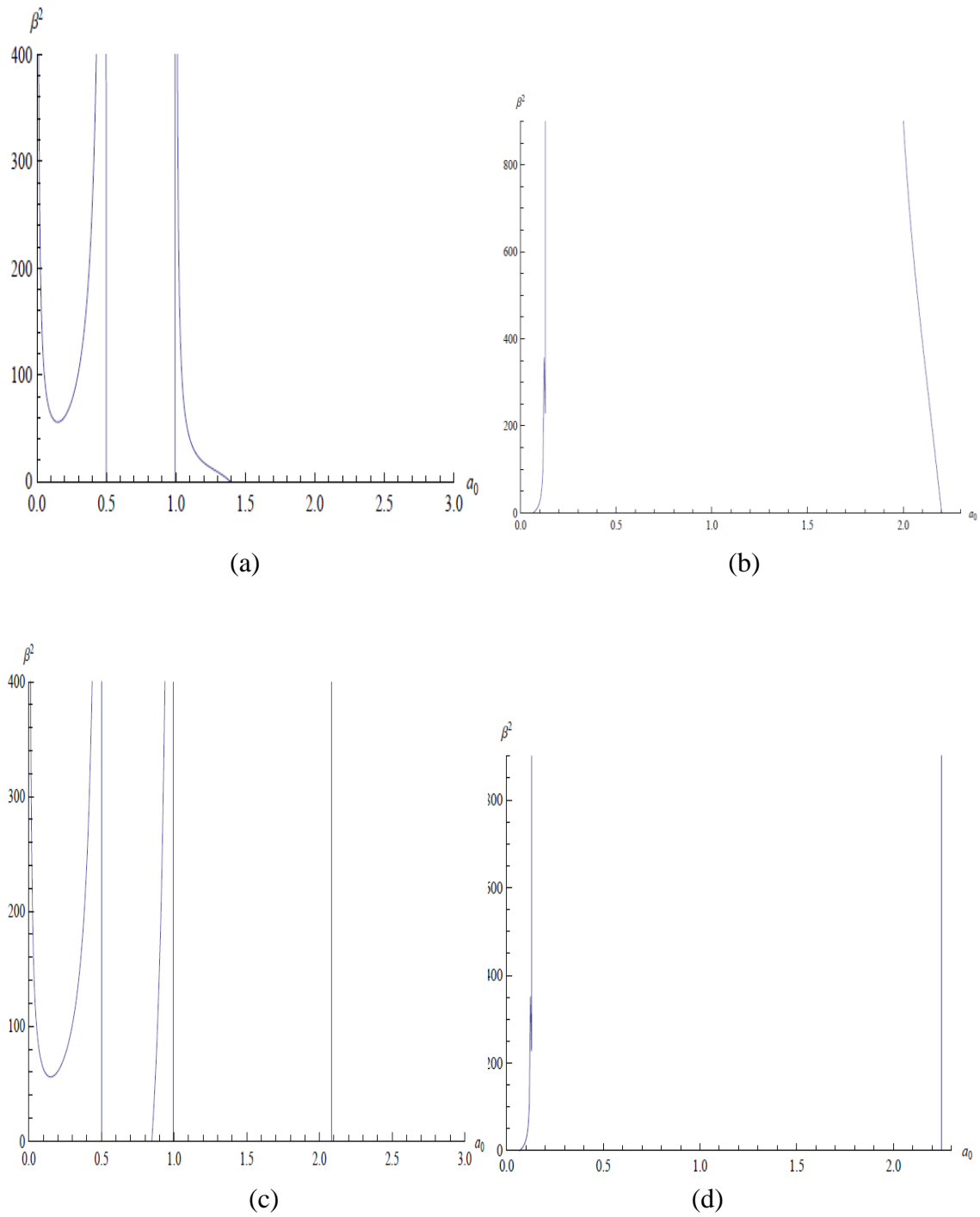
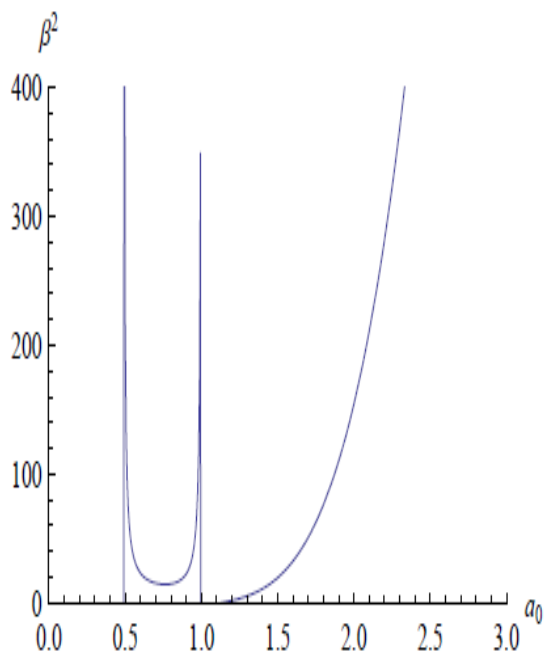
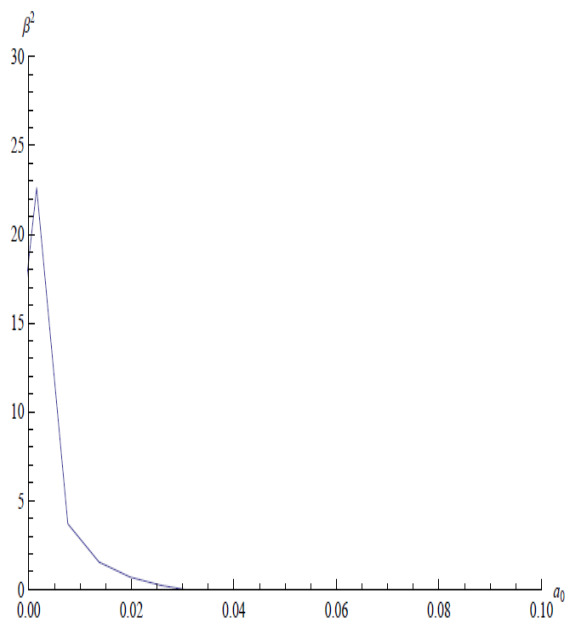


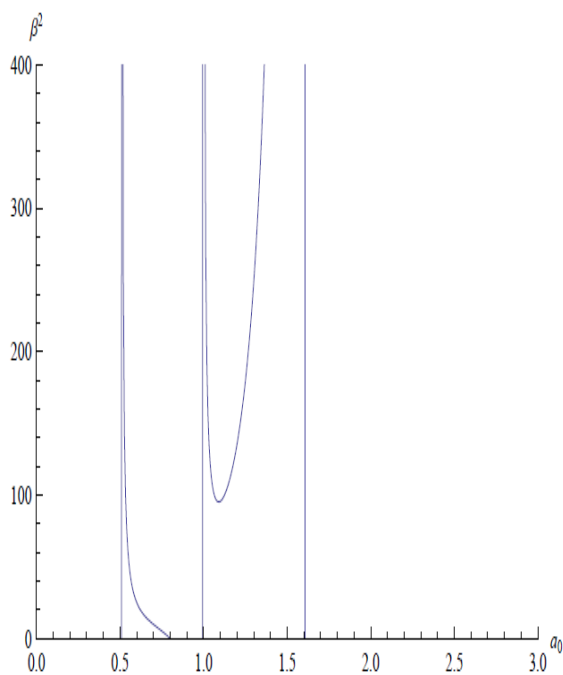
Figure 4. Stability regions TSW corresponding to $\omega = 0.4$ and the fixed value $m = 1$:
 (a) $\Lambda = -0.5, q = 1$, (b) $\Lambda = -0.5, q = 0.5$, (c) $\Lambda = 0.5, q = 1$, (d) $\Lambda = 0.5, q = 0.5$



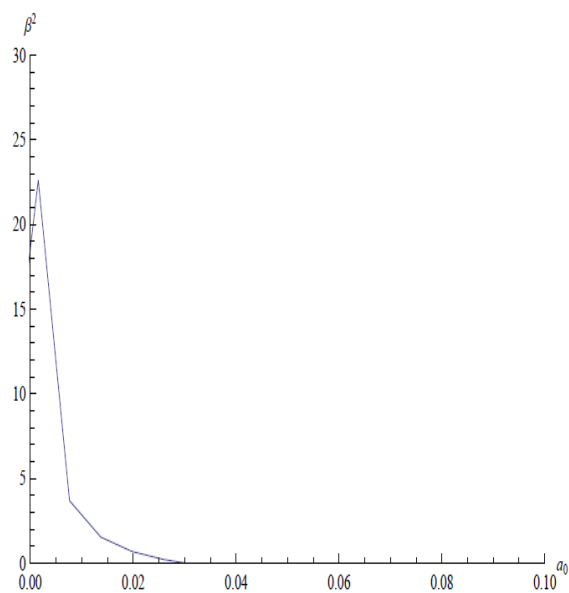
(a)



(b)



(c)



(d)

Figure 5. Stability regions TSW corresponding to $\omega = 2$ and the fixed value $m = 1$:
 (a) $\Lambda = -1, q = 1$, (b) $\Lambda = -1, q = 0.5$, (c) $\Lambda = 1, q = 1$, (d) $\Lambda = 1, q = 0.5$